Contents lists available at ScienceDirect

Biomedical Signal Processing and Control

DSP-based arrhythmia classification using wavelet transform and probabilistic neural network

Jose Antonio Gutiérrez-Gnecchi [a,*], Rodrigo Morfin-Magaña [a], Daniel Lorias-Espinoza [b], Adriana del Carmen Tellez-Anguiano [a], Enrique Reyes-Archundia [a], Arturo Méndez-Patiño [a], Rodrigo Castañeda-Miranda [c]

[a] Instituto Tecnológico de Morelia, Departamento de Ingeniería Electrónica, Avenida Tecnológico 1500, Morelia, Michoacán, Mexico
[b] CINVESTAV/IPN, Av. Instituto Politécnico Nacional 2508, Col. San Pedro Zacatenco, C.P. 07360 México, D.F., Mexico
[c] Universidad Autónoma de Zacatecas, Unidad Académica de Ingeniería Eléctrica, Jardín Juárez 147, Zacatecas, Mexico

ARTICLE INFO

ABSTRACT

A large part of the biomedical research spectrum is dedicated to develop electrocardiogram (ECG) signal processing techniques to contribute to early diagnosis. However, it is common to find that ECG analysis methods reported are confined to off-line PC host operation. The authors present an arrhythmia classification method implemented on a Digital Signal Processing (DSP) platform intended for on-line, real-time ambulatory operation to classify eight heartbeat conditions: normal sinus rhythm (N), auricular fibrillation (AF), premature atrial contraction (PAC), left bundle branch block (LBBB), right bundle branch block (RBBB), premature ventricular contraction (PVC), sinoauricular heart block (SHB) and supraventricular tachycardia (SVT). The algorithm uses a wavelet transform process based on quadratic wavelets for identifying individual ECG waves and obtain a fiducial marker array. Classification is conducted by means of a Probabilistic Neural Network. The algorithm is tested with 17 ECG records obtained from the PhysioNet repository. The proposed classification procedure was tested initially on MATLAB and the results where compared with the equivalent analogue data fed to a DSP-based ECG data acquisition prototype through an arbitrary waveform generator. The results derived from confusion matrix tests yielded on-line classification accuracy of 92.69% (AF), 97.15% (N), 76.82% (PAC), 91.06% (LBBB), 87.5% (RBBB), 71.04% (PVC), 91.94% (SHB) and 95.45% (SVT), overall classification rate of 92.746% and 100% agreement between the MATLAB and on-line DSP implementations. The results suggest that the method and prototype presented may be suitable for being implemented on wearable sensing applications auxiliary for on-line, real-time diagnosis.

1. Introduction

Cardiac arrhythmia occurs intermittently at early stages of heart disease which difficult early diagnosis. Undiagnosed cardiac arrhythmias often evolve undetected [1], reducing the effectiveness of treatment in advanced stages. In addition, tachyarrhythmic events are associated with sudden dead [2], occurring less than an hour after symptoms onset [3]. Thus, a large part of the biomedical research spectrum is directed towards developing electrocardiogram (ECG) diagnostic equipment and signal processing techniques [4] to contribute to early diagnosis so as to improve the effectiveness of heart disease treatment beginning at the early stages. On the other hand, current trends in ambulatory diagnostic equipment involve the use of remote implantable monitoring [5] and wearable sensing technologies [6] that may facilitate obtaining on-line real-time data for immediate, remote diagnosis. The advances in electronics technology during the last decade have contributed to the development of commercial, powerful mixed-signal data acquisition and processing devices, suitable for wearable sensor applications. Therefore methods for real-time cardiac arrhythmia detection for ambulatory data acquisition devices are continuously reported that may result in enhanced on-line detection of intermittent events that may otherwise be undetected. However, many ECG analysis results reported are confined to traditional, off-line, PC-based operation. Here, the authors address the importance of arrhythmia classification procedures intended for on-line operation and compare results obtained off-line with those processed through the DSP hardware developed for this application

* Corresponding author.
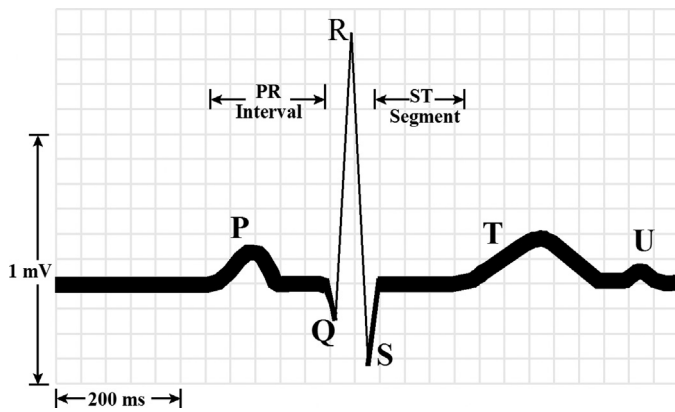E-mail address: biodsprocessing@aol.com (J.A. Gutiérrez-Gnecchi).

Fig. 1. Normal ECG pattern.

1.1. Arrhythmia classification procedures

The term arrhythmia is associated with changes of frequency, rhythm or morphology of the ECG signal in comparison with normal ECG values (Fig. 1).

In general, and in a very simplified manner, arrhythmia classification [7] from ECG graphical records involves 5 main steps:

(A) Calculate cardiac frequency. The heartbeat rate (HR) is considered normal between 60 beats per minute (bpm) and 100 bpm [8,9]. Based solely on HR, arrhythmias can be classified as bradyarrhytmias (HR < 60 bpm) and tachyarrhythmias (HR > 100 bpm). Cardiac frequency calculation is probably the easiest process that can be implemented on-line, and thus has become an integral part of ECG ASIC (Application Specific Integrated Circuits) hardware (i.e. Texas Instruments ADS129X series).

(B) Measure the RR interval. The R wave-to-R wave interval (RR) is an indicator of ventricular rate and should be regular with less than 0.12 s difference between heart beats.

(C) Examine the P wave. If the P wave precedes the QRS complex the impulse is generated in the SA node. The presence of abnormal locations of the P waves may indicate an ectopic pacemaker.

(D) Measure the PR Interval. The normal interval is considered between 0.1 and 0.2 s. A larger difference indicates a defect of the conduction system.

(E) Measure the QRS complex duration and morphology. If the width between the beginning of the Q wave and the end of the S wave is larger than 0.12 s, there may be an intraventricular conduction defect.

The steps outlined here do not intend to diminish in any way the complex nature of the ECG signal, but merely to serve as a starting point for highlighting some of the ECG prominent features that need to be analyzed that can lead to automated arrhythmia classification. In addition, the expertise of the specialist for analysing the graphical records, is a key factor in identifying heartbeat conditions related to specific cardiopathies.

Thus, achieving accurate automated arrhythmia diagnosis is a challenging goal that has to account for multiple heartbeat characteristics. For instance, supraventricular heart rhythm disorders include different types of arrhythmias, each one presenting different ECG signal signatures that defy the accuracy of detection and classification procedures. As an example, atrial fibrillation (AF) is considered the most common arrhythmia characterized by the absence of prominent P-waves often appearing as fibrillatory waves on the ECG record, and varying RR intervals. The prevalence of AF is of great interest for developing automated classification

methods so as to aid diagnosis. However, the difficulties to correlate the absence of P-waves and irregular RR intervals or existing P waves in chaotic heart rhythms can lead to misdiagnosed atrial fibrillation [10]. The inherent difficulty of identifying the ECG waves corresponding to AF may also lead to automated classifications errors [11]. Supraventricular tachycardia is another example of an abnormal heart rhythm where there is an increase in heartbeat rate and the P-wave overlapping the narrow QRS complex [12]. Thus, in automated ECG analysis, there are a number of preprocessing and signal component identification analysis procedures that need to be carried out prior to classification. Moreover, given the vast amount of information that can be derived from the ECG records, several methodologies have been, and continue to be proposed to try to correlate successfully, ECG signal deviations from the standard pattern to specific arrhythmia conditions (Table 1).

Thus, in general, there are three main processes involved in arrhythmia classifications procedures: ECG signal preprocessing, ECG wave component detection and classification.

1.1.1. ECG signal preprocessing

Since real ECG signals are noisy (i.e. white and mains noise) and contaminated with artefacts (i.e. electromyographic signals due to breathing and chest movement) the first step generally consists of bandpass filtering the measured signals. The choice of overall bandpass filter bandwidth as initial stage is a compromise; it should allow baseline (isoelectric) correction as well as noise reduction without losing high-frequency details that may be critical for individual wave identification [13]. The use of a wavelet denoising operation, prior to feature extraction, has been shown to preserve the sharp features of the ECG signal [14]. For instance, Chen et al. [15] use a wavelet denoising stage based on a discrete wavelet transform, with three levels of decomposition, as the first processing stage for real-time QRS complex detection. Thus a wavelet denoising operation appears to be suitable for on-line operation while maintaining the ECG features for further processing stages.

1.1.2. ECG feature extraction based on wavelet transform operations

The next step in ECG arrhythmia classification consists of identifying individual ECG wave components. Many analysis methods for automatic heartbeat classification have originated from QRS complex signal processing methods [16], because the QRS complex represents the most pronounced characteristic of the ECG signal. One of the techniques that has been favoured to identify individual ECG signal components is the wavelet transform (WT) using a variety of wavelet functions. Amongst the reported wavelet functions used for ECG component identification are the Haar wavelet [17,18], the Mexican hat wavelet [19,20], the Morlet wavelet [21,22] quadratic spline wavelet [23] and combination of wavelet functions [24].

In [13] the authors present a wavelet-based QRS complex detection algorithm on signals contaminated with simulated electromyographic noise which led to a series of results similar to those presented in traditional QRS detection [25,26] techniques. The authors in [27] present the use of the Haar discrete wavelet transform for QRS detection; their algorithm achieved a 95.74% detection accuracy rate on 5 test subject's data records, in comparison with the method presented in [28] which yielded an accuracy of 92.55%.

In [29] the authors use a cubic spline wavelet for detecting the QRS complex which resulted in a mean detection error of 0.75%. In [30], eight 30-min MIT/BIH database records were analyzed using a continuous wavelet transform procedure to detect the characteristic points of the QRS and T waves yielding a 0.47% false detection rate. QRS complex delineation is another type of algorithm aimed at

Table 1
Review summary of proposed ECG signal processing methods for filtering, feature extraction and arrhythmia classification.

Author and date	Type of ECG analysis	Processing function	Test conditions	Results
Okada (1979) [26]	QRS detection	Five-step digital filter	Data obtained from 4 patients in surgery	An overall detection rate better than 99.98% can be inferred
Pan and Tompkins (1985) [39]	Real-time QRS detection	Digital analysis of slope, amplitude and width of the signal for QRS detection. Bandpass filter to reduce false detections and adjustable parameter and threshold level to accommodate ECG changes as QRS morphology and heart rate	The authors use 48 MIT/BIH arrhythmia data base records	Achieved an overall 0.675% error detection rate
Hamilton and Tompkins (1986) [25]	QRS detection	Combination of linear and non-linear digital filters. Peak detector and QRS decision rules	48 records obtained from the MIT/BIH database records to test dedicated QRS detection hardware	Achieved 99.69% sensitivity and 99.77% positive predictivity
Sun et al. (1992) [40]	Real-time QRS detection	Comparison of nonlinear transformations and adaptive thresholding with respect to the Okada [26] method	The authors use 8 records obtained from the American Heart Association (AHA) database	The three point with sign consistency algorithm performance was similar to that of the Okada method. A set of conclusions for hardware implementation were given
Laguna et al. (1994) [36].	QRS, P and T waves in multilead ECG signals	Combination of methods including bandpass linear filter, low pass differentiator, moving-window integration, adaptation of the Pan and Tompkins [39] method for single-lead QRS detection. Decision rule for multi-lead QRS detection. Peak and zero crossing location and differentiated threshold	Tested using MIT/BIH database records. Validation of the procedure using the CSE database	Algorithm yields measurements with standard deviations compared to those made by human specialists
Li et al. (1995) [44]	QRS, P and T waves	Quadratic spline wavelet	The authors use 46 data records obtained from the MIT/BIH database	The WT algorithm produced a 99.8% QRS complex detection accuracy
So and Chan (1997) [28]	QRS detection	Digital filter, maximum slope detection based on first derivative method	Algorithms tested on 20 American Heart Association (AHA) records	Reduced accuracy in comparison to other methods but simpler, so it is possible to implement for on-line operation
Kadambe et al. (1991) [13].	QRS detection	Cubic spline with centre frequency at 120 Hz and 204 Hz bandwidth to implement the Dyadic Wavelet Transform (Dy WT)	Tested on the American Heart Association database (80 dual channel ECG data tapes)	Results similar to other techniques (Hamilton-Tompkins [25], Okada [26], MOBD [40])
Dinh et al. [29].	QRS detection	Cubic spline wavelet	The authors use the first four-minute signals of 25 records obtained from the MIT/BIH database	Reduced mean detection error values of 0.75%
Homaeinezhad et al. (2001) [37].	QRS complex geometrical feature extraction applied to heartbeat classification	Combination of quadratic spline wavelet and Fuzzy inference classification	Method tested using 12 MIT/BIH database records to classify 4 heartbeat conditions	Algorithm yielded a 94.58% (FCM clustering) and 97.41% accuracy (fuzzy classifier based on subtractive clustering)
Burke and Nasor (2002) [20]	ECG components detection	Mexican Hat Wavelet	Used data from 21 healthy subjects aged between 13 and 65 years old to examine timing relationships of ECG components	Characterization of each component timing variation by polynomial approximation
Schuck and Wisbeck (2003) [21]	QRS detection	Complex Morlet wavelet function	25 record obtained from the MIT/BIH database. Software coded in MATLAB	Improved results in comparison with those obtained by preprocessing the signal according to the Pan & Tompkins [39] and Hamilton & Tompkins [25] method
Alexakis et al. (2003) [38]	Detection of delayed ventricular repolarisation based on five ECG features (RR, RTc, T wave amplitude, T wave skewness and T wave kurtosis)	Performance comparison between Artificial Neural Network (ANN) (multilayer perceptron) and Linear Discriminant Analysis (LDA)	ECG records and corresponding blood glucose levels obtained from eleven type-1 diabetic patients	The ANN method yielded a maximum accuracy of 87.5% whereas the LDA method maximum accuracy was 89.96%
Martínez et al. (2004) [31]	QRS detection and ECG delineation	Quadratic Spline wavelet	The authors conduct an extensive test programme on 48 MIT/BIH, 105 QT, 90 European ST-T data set 3 (125 files) of the CES multilead measurement database	Obtained a 99.66% sensitivity and positive predictivity of 99.56% using the European ST-T and CSE databases. The results using the MIT/BIH database resulted in sensitivity and positive predictivity better that 99.8%
Atoui et al. (2004) [33]	12-lead ECG synthesis	Compares the results of using a multi-layer feedforward artificial neural network with supervised training and a multiple regression-based analysis method	The authors use over 300 data record from adult patients	The root mean square error and correlation coefficients obtained using the ANN method were better that those of the regression method suggesting that an ANN approach can be used to synthesize ECG signals

de Chazal et al. (2004) [35]	Classification of 5 heartbeat conditions (normal beat, ventricular ectopic beat, supraventricular ectopic beat, fusion of a normal and ventricular ectopic beat and unknown beat type)	Preprocessing using a median filter, manually allocated fiducial points for heartbeat detection, segmentation based on the Laguna et al. method [36] and feature extraction by calculating features separately relating to heartbeat intervals	44 nonpeacemaker recordings from the MIT/BIH database	The proposed independent performance assessment yielded a sensitivity of 75.9%, a positive predictivity of 38.5%, and a false positive rate of 4.7% for the SVEB class. For the VEB class, the sensitivity was 77.7%, the positive predictivity was 81.9%, and the false positive rate was 1.2%
Gutiérrez et al. (2005) [17].	QRS detection	Haar wavelet	Tested on 25 MIT/BIH records and 48 European ST-T records	Achieved figures of 1.19% and 0.19% error on MIT/BIH and ST-T records respectively
Alvarado et al. (2005) [30].	QRS and T wave detection	Continuous spline wavelet transform	8 records obtained from the MIT/BIH database were used to evaluate the algorithm	The authors obtained an average 0.47% detection error
Tsipouras et al. (2005) [34].	Arrhythmia classification based on RR-interval identification using knowledge-based methods	Low order polynomials for preprocessing (baseline correction), Hamilton and Tompkins-based algorithm for QRS detection and RR-interval signal computation. A set of rules for arrhythmic beat classification using a 3 RR-interval window. Deterministic automaton for arrhythmic episode detection and classification	48 ECG records obtained from the MIT/BIH database	The method resulted in 98% accuracy for arrhythmic beat classification and 94% accuracy for arrhythmic episode detection and classification
Chen et al. (2006) [15].	QRS detection	Moving average (Daubechies 4 Wavelet for signal denoising)	45 patient record obtained from the MIT/BIH database. Software coded in MATLAB	Reduced computational time to complete one analysis procedure (1.5 ms) on an Intel processor-based PC. Achieved 99.5% detection rate
Lin et al. (2008) [45]	Classification of 7 heartbeat conditions: normal beat, supraventricular ectopic beat, bundle branch ectopic beat, and ventricular ectopic beat	Combination of Morlet Wavelet function and Probabilistic Neural Network (PNN)	Data extracts from MIT/BIH database	The classification accuracy is high (up to 100%) when a single arrhythmia is presents but degrades when multiple arrhythmias are present
Kaneko et al. (2011) [18]	QRS classification	Combination of Haar wavelet and Self Organizing Map (SOM)	16 records obtained from the MIT/BIH database	Improved results classifying 5 beat conditions in comparison to other (cross-correlation, FFT and only SOM methods)
Ieong et al. (2012) [23].	QRS detection	Quadratic Spline wavelet	48 records obtained from the MIT/BIH database records to test dedicated QRS detection hardware	The dedicated hardware showed high sensitivity (99.31%) and predictivity (99.70%) in real-time tests
Jaswal et al. (2012) [27]	QRS detection	Haar wavelet	Data obtained from 5 subjects. 94 beats analyzed	Improved detection accuracy values of 95.74% in comparison with results analyzed using the So and Chan [28] method (92.55%)
Manikandan and Soman (2012) [32]	R-peak detection	Combination of Hilbert Transform and moving average filter	48 records obtained from the MIT/BIH database records	Achieved 99.80% average detection rate, 99.93 sensitivity and 99.86% positive predictivity
Zeng et al. (2013) [24]	QRS detection	Combination of Mexican-hat and Morlet Wavelets	10 records obtained from the MIT/BIH database	Achieved 99.71% of detection sensitivity and 99.53% positive prediction values
Ebrahimnezhad and Khoshnoud (2013) [46]	Classification of 4 heartbeat conditions: Normal sinus rhythm, Atrial premature contraction (APC), Right bundle branch block (RBBB) and Left bundle branch block (LBBB)	Combination of Linear predictive coefficients and Probabilistic Neural Network	The authors use 48 data records obtained from the MIT/BIH database	The method yielded 92.9% accuracy and 93.17% sensitivity
Yu and Chen (2007) [47]	Classification of 6 heartbeat conditions: normal beat (N), the left bundle branch block beat (LBBB), the right bundle branch block beat (RBBB), atrial premature beat (APB), premature ventricular contraction (PVC), and paced beat (PB)	Haar wavelet transform and Probabilistic Neural Network	The authors use 23 records from the MIT/BIH database	The authors obtained a 99.65% accuracy detecting 6 heartbeat conditions
Vassilikos et al. (2014) [22]	QRS feature analysis	Complex Morlet wavelet function	Analysis of 38 records obtained from patients with ischaemic (39%) and non-ischaemic (61%) cardiomyopathy	Found that QRS analysis based on Morlet-based wavelet is a better predictor of response to cardiac resynchronization therapy (CRT) than QRS duration

identifying peaks, beginning and end of P and T waves [31]. In [25] the authors use a wavelet transform process to delineate the QRS complex by peak detection. In [32] the authors address the issue of the non-stationary nature of the QRS morphology for R-peak detection and propose a combination of the Hilbert transform (HT) and moving average (MA) filter to yield a 99.80% average detection rate on 48 MIT ECG records.

1.1.3. Arrhythmia classification process

Once individual wave components have been identified, the results are transferred to a classifier process. The authors in [33] use a multilayer, 3-input neuron, feedforward artificial neural network trained with supervised backpropagation; the results using 1-second data extracts from 10-second registers sampled at 1 ksps (kilosamples per second) were better than those obtained using multiple regression analysis. The authors in [34] explore the use of the RR-interval for arrhythmia classification using knowledge-based methods to classify four heartbeat conditions (normal, premature ventricular contractions, ventricular flutter/fibrillation and 2nd heart block) and six rhythm types (ventricular bigeminy, ventricular trigeminy, ventricular couplet, ventricular tachycardia, ventricular flutter/fibrillation and 2nd heart block), yielding a 98% accuracy for arrhythmic beat classification and 94% accuracy for arrhythmic episode detection and classification.

The authors in [35] use the programme of Laguna et al. [36] to feed manually allocated detected heartbeats in one of the five beat classes recommended by ANSI/AAMIEC57:1998 standard, resulting in a sensitivity of 75.9%, a positive predictivity of 38.5%, and a false positive rate of 4.7% for the supraventricular ectopic beat (SVEB) and a sensitivity of 77.7%, positive predictivity 81.9%, and false positive rate of 1.2% for unknown beat type. In [18] the authors present an automated classification method using the Haar wavelet transform and a two-layer Self Organizing Map (SOM) to classify five heartbeat conditions and compare the results with cross-correlation coefficient, single layer classification method with power spectrum and two layered SOM classification with time domain parameters. The results yielded 0.39% classification error rate for WT-SOM combination in comparison with 0.82% error rate obtained using the correlation coefficient method. Homaeinezhad et al. [37] reports the results of combining a QRS complex geometrical feature extraction technique and fuzzy network classifier to classify four heartbeat conditions (Normal, Left Bundle Branch Block (LBBB), Right Bundle Branch Block (RBBB), Paced Beat (PB)) in 12 MIT/BIH records yielding accuracies of 94.58% and 97.41% for Fuzzy C-means and subtractive clustering-based fuzzy-logic classifiers, respectively. In [38] the authors compare the results of using a multilayer perceptron artificial neural network (MLP-ANN) and Linear Discriminant Analysis (LDA) to detect delayed ventricular repolarisation based on five ECG features (RR, RTc, T wave amplitude, T wave skewness and T wave kurtosis) and resulted in 85.07% detection accuracy using the ANN method and 89.96% accuracy using the LDA method. The importance of real-time signal wave identification [39] based on microprocessing units [40] has been addressed for over 3 decades and has resulted in continuous proposal and evaluation of different methodologies [41]. In [17] the authors consider on-line implementation of QRS complex detection based on Haar Wavelet transform resulting in 1.19% and 0.19% error when evaluating 24 MIT/BIH and 48 ST-T database records respectively. In particular the Probabilistic Neural Network (PNN) Classifier has been suggested to be suitable for implementation on dedicated processing hardware, due to acceptable time and frequency resolution when applied to ECG analysis. The authors in [42] present a MATLAB programme to explore the feasibility of using a combination of bump function and probabilistic Neural Network to classify eight heartbeat conditions using 17 MIT/BIH records.

2. Methods

In general terms, the classification task consists of obtaining the wavelet transform of a 6-second segment portion of the ECG record to obtain the fiducial marker (detection and location of single wave components) and feature arrays to feed the Probabilistic Neural Network. However, as outlined in Section 1.1, the procedure involves several operations in each of the three processing stages: preprocessing, signal processing for feature extraction and classification (Fig. 2).

2.1. Wavelet transform (WT)

The wavelet transform is used to obtain a time-frequency component representation in different bandwidths. Consider a function of real or complex values, $\Psi(t)$, in Hilbert space $L^2(R)$, where L represents the vector space of square-integrable functions, with zero mean (1):

$$\int_{-\infty}^{+\infty} \psi(t)dt \tag{1}$$

and square norm one (2):

$$\int_{-\infty}^{+\infty} \left| \psi(t) \right|^2 dt \tag{2}$$

A family of wavelet functions is obtained from (3):

$$\psi_{u,s}(t) = \frac{1}{\sqrt{|s|}} \psi\left(\frac{t-u}{s}\right) \tag{3}$$

where s represents the scale factor contracting ($s < 1$) or expanding ($s > 1$) the wavelet function. The translational factor u is used to shift the location of the wavelet function. The term $s^{-1/2}$ is an energy normalization parameter across the different scales.

Thus, the continuous WT representation of function $f(t) \in L^2(R)$ (4):

$$W_f(u, s) = f * \psi_{u,s}^* = \int_{-\infty}^{+\infty} f(t) \frac{1}{\sqrt{s}} \psi^*\left(\frac{t-u}{s}\right) dt \tag{4}$$

Scaling the translational factor allows separating the signal components into frequency ranges or scales. In order to implement the WT on a digital signal processing platform to process real data, it is necessary to utilize a fast discrete transformation. Given the scale factor $s = 2^j$ where $j \in \mathbf{Z}$, and $\mathbf{Z}$ is the set of all integers, yields the binary or dyadic wavelet transform [43]; choosing the translational and scaling factors to be multiples of two, results in a discrete binary wavelet transform implementation suitable for digital signal processing applications. The discrete wavelet transform of a digital signal $f(n)$ can be obtained from (5) and (6):

$$S_{2^j}f(n) = \sum_{k \in Z} h_k S_{2^{j-1}}f(n - 2^{j-1}k) \tag{5}$$

$$W_{2^j}f(n) = \sum_{k \in Z} g_k S_{2^{j-1}}f(n - 2^{j-1}k) \tag{6}$$

where $s_2^j f(n)$ are approximation coefficients, $W_2^j f(n)$ represent detail coefficients (2^j scale wavelet transform of $f(n)$) and n is the sample number. The terms $\{h_k, k \in \mathbf{Z}\}$ and $\{g_k, k \in \mathbf{Z}\}$ correspond to low pass coefficients ($H(\omega)$) (7):

$$H(\omega) = \sum_{k \in Z} h_k e^{-ikw} \tag{7}$$

and high pass coefficients ($G(\omega)$) respectively (8):

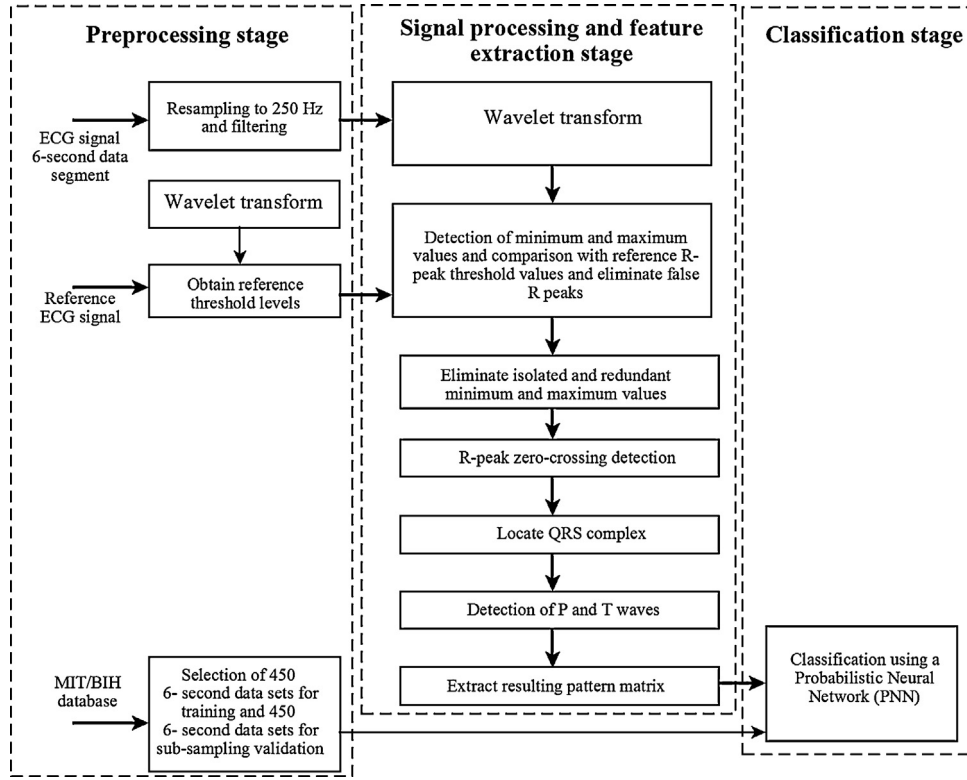$$G(\omega) = \sum_{k \in Z} g_k e^{-ikw} \tag{8}$$

Fig. 2. Block diagram of the ECG arrhythmia classification operation.
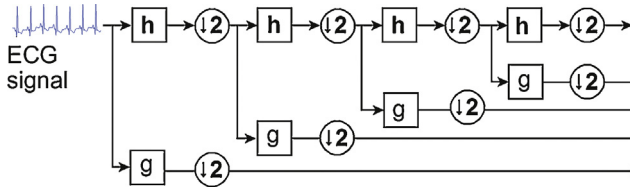

Fig. 3. The Mallat filter bank implementation.

The wavelet process used here is based on a quadratic wavelet function with Fourier Transform [50]

$$\Psi\left(\Omega\right) = i\Omega\left[\frac{\sin\left(\frac{\Omega}{4}\right)}{\left(\frac{\Omega}{4}\right)}\right]^4 \tag{9}$$

The filters are implemented as (10) and (11) [31,44]:

$$H(\Omega) = e^{\frac{i\Omega}{2}}\left(\cos\left(\frac{\Omega}{2}\right)\right)^3 \tag{10}$$

$$G(\Omega) = 4ie^{\frac{i\Omega}{2}}\left(\sin\left(\frac{\Omega}{2}\right)\right) \tag{11}$$

and thus

$$h[n] = \left(\frac{1}{8}\right)\left\{\delta\left[n+2\right] + 3\delta\left[n+1\right] + 3\delta\left[n\right] + \delta\left[n-1\right]\right\} \tag{12}$$

$$g[n] = 2\left\{\delta\left[n+1\right] - \delta\left[n\right]\right\} \tag{13}$$

The DWT computation of is conducted with a filter bank as described by Mallat [51] (Fig. 3).

2.2. ECG signal denoising

Prior to commence the individual ECG wave identification, it is necessary to perform other digital signal processing operations. The original ECG record (Fig. 4A), is displaced from the base line due to multiple effects.

The first processing step consists of restoring the baseline using wavelet denoising process as described elsewhere [42]. The restored signal is then resampled to 250 Hz, and band-reject filtered to reduce the effect of the mains (50 or 60 Hz, selectable).

The signal wave identification procedures require establishing a set of threshold values. The preprocessing stage also includes applying the Wavelet Transform to a reference ECG signal to obtain, off-line, the threshold values (Fig. 4B).

2.3. Individual ECG wave identification

The WT coefficients for feature extraction accommodate four scales; each scale corresponds to a predefined bandwidth: 62–125 Hz, 18–60 Hz, 8–26 Hz and 4–13 Hz (Fig. 5B). Detection and localization of R peaks is performed using the first three scales of the wavelet transform based on the detection of maximum and minimum values. Location of Q and S waves is based on detecting local maximum and minimum values that do not exceed thirty percent of the maximum threshold value nearest to the R peak. P and T wave detection is performed on the fourth scale because they are lower frequency waves. An identifier mark is assigned at the beginning and at the end of each ECG wave detected (Fig. 5C).

The identification of individual ECG waves and the classification can be summarized in seven main steps:

(a) *Heartbeat identification.* Heartbeat identification is based on detecting the maximum and minimum values at the different scales. Considering that $W_2^j f(\tau_0)$ is a minimum or maximum, $W_2^j f(\tau)$ is the largest magnitude from left to right and $W_2^j f(\tau')$ is the largest magnitude of the opposite side, if $\left|W_2^j f(\tau_0)\right| >$
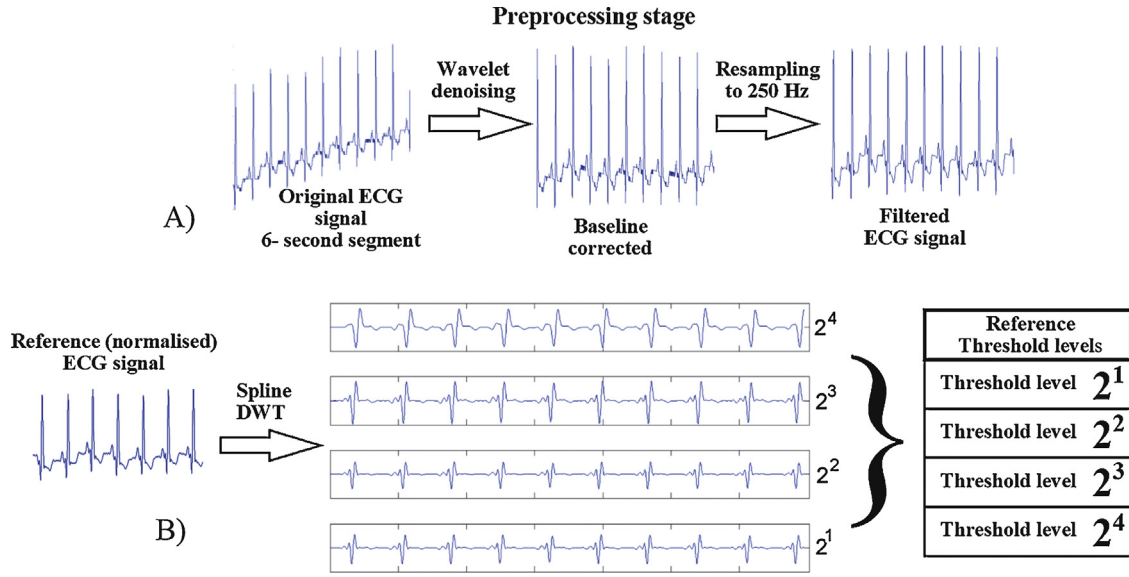
Fig. 4. Preprocessing the ECG signal includes performing (A) signal denoising and resampling operations to prepare the ECG signal for feature extraction and (B) obtaining the threshold reference values in the four scales.

$\left| W_2^j f(\tau) \right|$ and $\left| W_2^j f(\tau_0) \right| > \left| W_2^j f(\tau') \right|$ then $W_2^j f(\tau_0)$ is a minimum or maximum [44].

(b) *R wave identification*. After the maximum and minimum values have been determined, a threshold value is used to detect the R wave occurrence along the four wavelet scale results. Since the magnitude is not constant, a dynamically adjustable threshold value is used to obtain four localization group sets (14):

$$\left\{ n_k^4, n_k^3, n_k^2, n_k^1 \quad k = 1, \ldots, N \right\} \tag{14}$$

Fig. 5. Wavelet transform and ECG wave location. (A) Original ECG signal, (B) results of the wavelet transform and (C) individual wave identification processes.

where the superindex typographical mark indicates the wavelet transform scale and the subindex mark corresponds to the kth maximum detected.

(c) *Eliminate false R peaks*. Although the dynamic thresholding operation serves as a first way of reducing false R peaks, there may be some artefacts that resulted in false maximum values. Since not all the maximum points detected may correspond to an R peak, it is necessary to remove false R peaks. Consider that, within a time interval of 120 ms [44], there are two maximum negative values, NEG_1 and NEG_2, with absolute value A_1 and A_2, and two maximum positive values namely L_1 and L_2. The decision rule to remove false R peaks can be summarized as:

$$\text{if} \quad \frac{A_1}{L_1} > 1.2 \frac{A_2}{L_2} \quad \therefore NEG_2 \text{ is redundant} \tag{15}$$

$$\text{if} \quad \frac{A_2}{L_2} > 1.2 \frac{A_1}{L_1} \quad \therefore NEG_1 \text{ is redundant} \tag{16}$$

If NEG_1 and NEG_2 reside on the same side of the positive vale, the negative value further away is considered redundant. The process is repeated until the number of detections is even and coincides with the number of negative values.

(d) *Locate the R peak*. The R peak can be located from the pair maximum-minimum zero-crossings. In [44] the authors propose the use of scale 2^1 to detect the R peak position. However, when the signal contains electromyographic noise there may be more than a single zero-crossing occurrence detectable in scales 2^1 and 2^2. In addition ECG baseline drift can modify the zero-crossing location in scale 2^4. Therefore, the scale used for R peak location is 2^3.

(e) *Detection of the beginning and end of the QRS complex*. The detection process uses a window of 120 ms on each side of the R peak detected. The beginning of the QRS complex candidate is the first local maximum before an R peak and the end is the first minimum after an R peak. In the case where there is not an S wave component detectable, the search is extended until the extreme on the R peak is reached.

(f) *Detection of T and P waves*. Li et al. [44] review the results of Thakor et al. [52] to identify the energy content of the P and T waves in the frequency range from 2 Hz to 13 Hz. However in the range of 2–6 Hz the baseline drift is considerable and thus select the 2^4 scale for P and T wave identification. Therefore,
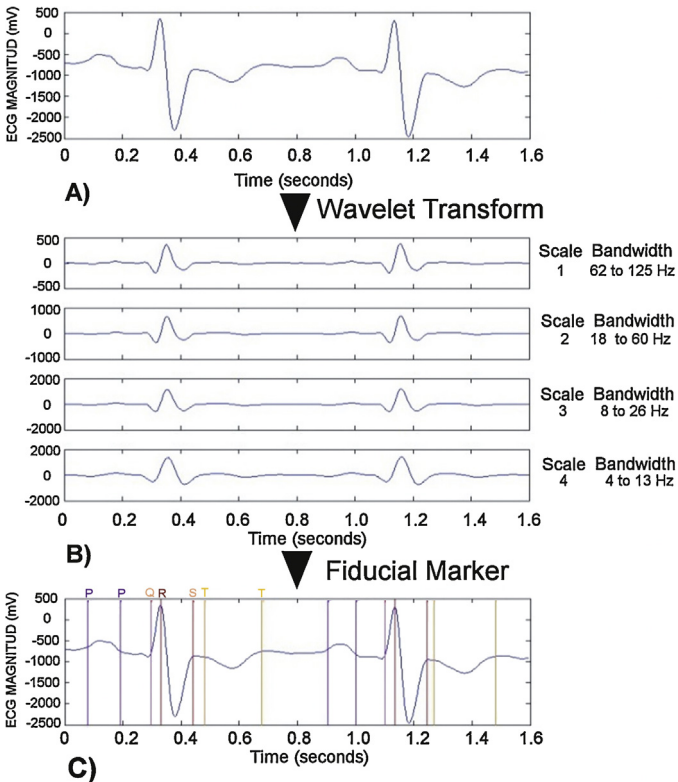
Table 2
Parameters obtained from each heartbeat.

Parameter	For each beat
Number of P waves	0,1,2,. . .
P wave polarity	−1 negative, 1 positive0 more than 1 P wave
QRS duration	Time (s)
PR interval	Time (s)
Position of R	Referenced to the beginning of the segment
RR interval	Time (s)
HR	Beats/minute
Global rhythm	0 abnormal, 1 normal

Table 3
Assignment of heartbeat classification identifier.

Heartbeat condition	Class
Auricular fibrillation (AF)	1
Normal sinus rhythm (N)	2
Premature atrial contraction (PVC)	3
Left bundle branch block (LBBB)	4
Right bundle branch block (RBBB)	5
Premature ventricular contraction (PVC)	6
Sinoauricular heart block (SHB)	7
Supraventricular tachycardia (SVT)	8

the P and T waves are sought in the fourth scale in the range between two QRS complexes. Once the QRS complex has been identified, in a similar manner to that presented in [31], the procedure uses a search window defined by the end of a QRS complex and the beginning of the next QRS complex.

(g) *Feature extraction*. Once individual waves have been located, a set of features for each heartbeat is obtained, and the results for the data segment are stored in an array (Table 2). The resulting feature array feeds the Probabilistic Neuronal Network which determines the probability of an arrhythmia detected by the algorithm: N, AF, PAC, LBBB, RBBB, PVC, SHB and SVT.

2.4. ECG arrhythmia classifier based on Probabilistic Neural Network (PNN)

Amongst the classifiers reported, the use of PNN classifiers has received considerable attention. In [45] the authors report up to a 100% success detection rate for single arrhythmia (PVC) although the classification accuracy diminishes (94%) when two or more heartbeat conditions are present. In [46] the authors obtained a 92.9% classification success rate of four types of heartbeat conditions using PNN and linear prediction coefficients. The authors in [47] reported a 99.65% success rate for six heartbeat conditions. Here the authors transfer the results obtained from the single-wave identification procedure to a PNN classifier (Fig. 6).

The PNN architecture is basically a backpropagation network with an activation function derived from statistical data. The pattern and classes layers require supervised knowledge to connect each pattern layer node to the corresponding class layer node. The aim is to cl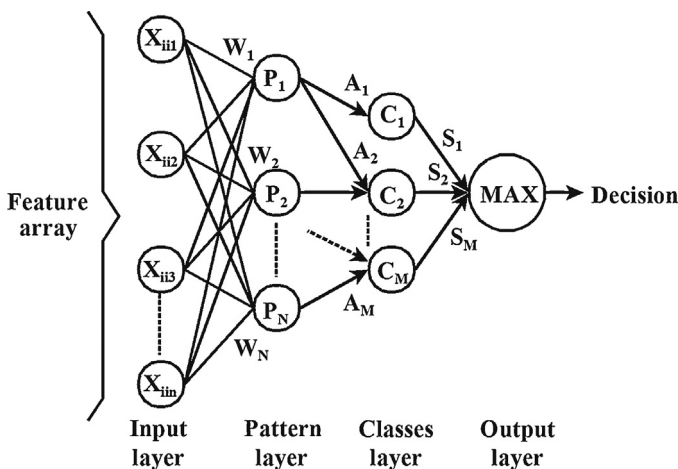assify the nth dimension feature vector X_{ii}, according to some predefined class C_M. A common procedure normalizes the weights, $WPNN_{kk}$, as (17):

$$WPNN_{kk} = \frac{x_{kk}}{x_{kk}} \quad k = 1, 2, \ldots, N \tag{17}$$

where $WPNN_{kk}$ corresponds to the P_{kk}th node, and $X_{kk} \neq X_{ii}$ is the training vector. The P_{kk} pattern layer output, O_{kk}, is (18):

$$O_{kk} = e^{\left(\frac{Z_{kk}-1}{\sigma^2}\right)} \tag{18}$$

where the width of the Gaussian function, σ, is selected to control the exponential activation function scale factor. O_{kk} is the exponential kernel result operating over the dot product between the kkth training vector and the X_{ii} vector to be classified, Z_{kk} (19):

$$Z_{kk} = W_{kk}^T \frac{X_{ii}}{X_{ii}} \tag{19}$$

The A_M functions are defined as (20):

$$A_{M_{kk}} = \begin{cases} 1 & W_{kk} \in C_M \\ 0 & otherwise \end{cases} \tag{20}$$

and the S_M array contains the equivalent proportional probability estimates (21):

$$S_M = \sum_{kk=1}^{N} O_{kk} A_{M_{kk}} \tag{21}$$

Classes are assigned per type of heartbeat condition (Table 3).

2.5. Training the probabilistic neural network

There are a number of techniques that may be used for training the Neural Network. When the available data includes even amounts of data sets with similar characteristics, it is possible to apply clustering techniques to avoid overfitting. However, the amount of each type of heartbeat condition of interest for this work, differ in the chosen MIT/BIH database records. The overall ratio of arrhythmic data segments to normal beat data segments in the records chosen, is more than 30% where atrial fibrillation is predominant (∼14%) and other heartbeat conditions not considered for this work also have a large ratio in comparison with, for instance, SVT. Incidentally, the smallest percentage corresponds to SVT (<0.5%). Thus it is not possible to use cross-validation methods effectively since there is an uneven number of heartbeat conditions.

After testing different ratios of training and testing datasets, the authors obtained the best training performance by individually selecting 450 6-s segments, to ensure that the training data set includes all the target heartbeat conditions. Testing for sub-sampling validation was conducted by selecting a different set of 450 6-s data segments, ensuring that all the target heartbeat conditions are included. The training data set corresponds to approximately 10% of the total number of data sets analyzed. Table 4 shows the results of the training procedure.

Fig. 6. Probabilistic neural network (PNN) classifier.

Table 4
Summary of PNN training test results.

Heartbeat condition included in the test data set	Number of segments for training	Number of segments for testing	Correctly classified		False negatives		False positives	
			#	%	#	%	#	%
Auricular fibrillation	45	45	44	97.78	1	2.22	0	0.00
Normal sinus rhythm	195	195	194	99.49	0	0.00	1	0.51
PAC	45	45	45	100.00	0	0.00	0	0.00
LBBB	45	45	45	100.00	0	0.00	0	0.00
RBBB	45	45	43	43.00	2	4.44	0	0.00
PVC	45	45	44	97.78	1	2.22	0	0.00
SHB	20	20	20	100.00	0	0.00	0	0.00
SVT	10	10	10	100.00	0	0.00	0	0.00
Total	450	450	445	98.89	4	0.89	1	0.22

#: number of 6-s data segments.
%: percentage referenced to the total number of segments per heartbeat condition.
False negatives: normal beat detected when there is an arrhythmic condition.
False positives: abnormal beat detected when there is a normal sinus rhythm.

2.6. Confidence factor (CF)

The classification results are issued a classification confidence factor (CF) (22):

$$CF = 1 - e^{\left(\frac{P_1 - P_2}{P_2}\right)} \qquad (22)$$

where P_1 is the highest probability and P_2 is second highest probability obtained from the PNN process.

2.7. Digital Signal Processor-based hardware for ECG arrhythmia classification

The algorithm described in Sections 2.2 and 2.3 was initially implemented in MATLAB (Mathworks) to allow rapid functional verification. Once the procedures were tested in the host PC, a dedicated hardware platform was developed to test the on-line performance of the algorithm. Fig. 7 shows the schematic diagram of the DSP-based hardware implemented for this application.

An arbitrary waveform generator (Agilent Technologies) is used to generate the test signal derived from the digitized PhysioNet [48,49] records (Fig. 7A). The resulting analogue signal (Fig. 7B) is fed to a medical analogue front-end integrated circuit (ADS1293) to acquire and digitize the test signal (Fig. 7C). The data acquisition process is controlled by means of a DSP (digital signal processor) integrated circuit (TMS320C5535) (Fig. 7E) through an SPI interface connection (Fig. 7D). The prototype includes an LCD display (Fig. 7F) and push-button keyboard (Fig. 7G) to operate the device in stand-alone operation. The acquired data can be either stored on micro-Secure Digital (SD) memory card (Fig. 7H) and/or transferred to the host PC through an USB connection. Data can be on-line analyzed or transferred to the PC for further analysis and permanent storage (Fig. 7I). The DSP arrhythmia classification procedure was implemented in C++ programing language using the Code Composer Studio™ development suite (Texas Intruments-Spectrum Digital). The C++ programme includes several functions to allow stand-alone operation and data transfer to a host PC for further analysis, performance comparison and permanent storage.
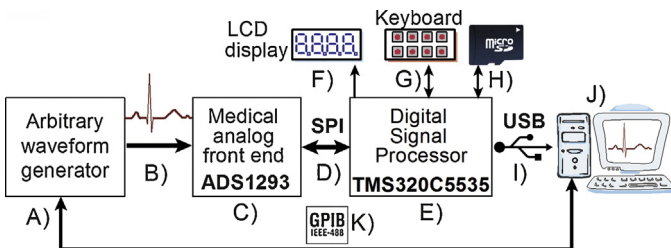
1. **Welcome screen**
2. **Continuous monitoring**
3. **Holter mode (Continuous recording)**
4. **Data transfer**
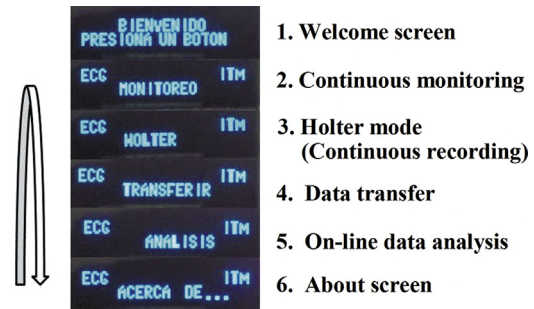5. **On-line data analysis**
6. **About screen**

Fig. 8. Summary of operations accessible through a rotating menu.

The user interface LCD screen displays a navigation menu to access the operating functions (Fig. 8).

In continuous monitoring mode the data is transferred directly to the PC. A host programme developed in MATLAB, receives, plots and stores the measured data when the device operates in continuous mode. The reason to implement the host programme in MATLAB is to ease the prototype performance comparison with that of the MATLAB implementation. In Holter operation, the device samples and stores the incoming data in the SD memory card. Every measurement is stored as 32-bit data. In data transfer mode, the last Holter operation data stored in non-volatile (SD) memory is transferred to the PC. The MATLAB programme also receives the SD data for permanent storage into a spreadsheet file.

Before continuous operation can begin, it is necessary to perform two operations: calculation of threshold coefficients based on a reference ECG signal and training the neural network. Both processes are performed off-line and the results are transferred to the DSP memory. In on-line operating mode data is sampled at 500 samples per second to acquire a 6-s data set. Once the entire signal analysis feature extraction and classification procedures are performed, the classification results are shown on the LCD screen and the process is repeated for the next 6-s data set until stopped by the user.

3. Experimental procedure

The availability of the MIT/BIH database has been an invaluable tool for developing ECG signal processing algorithms and permits performance comparison. The algorithm developed for this application was tested using seventeen 30-min ECG lead II (DII) data registers from the PhysioNet repository [48]: 100, 101, 103, 105, 106, 118, 119, 201, 202, 203, 205, 207, 209, 210, 213, 215 and 219. The original PhysioNet records, sampled at 360 Hz, are downsampled at 250 Hz. The resulting data is scaled to accommodate

Fig. 7. Schematic diagram of the experimental setup.

Table 5
Summary of example test results: record 118, time frame 78–84 s.

Evaluated parameters	Parameter values per heartbeat detected on segment						Vector feature
	1st	2nd	3rd	4th	5th	6th	
A. Number of P waves	1	1	1	1	1	1	2
B. Polarity of P	1	1	1	1	1	1	5
C. QRS duration	0.144	0.136	0.144	0.144	0.14	0.144	2
D. PR interval	0.2	0.196	0.216	0.196	0.204	0.216	2
E. R Location	1.092	1.92	2.372	3.536	4.368	5.196	
F. RR interval	0.812	0.828	0.812	0.804	0.832	0.828	
G. Heartbeat rate	70						2
H. Rhythm	1						1
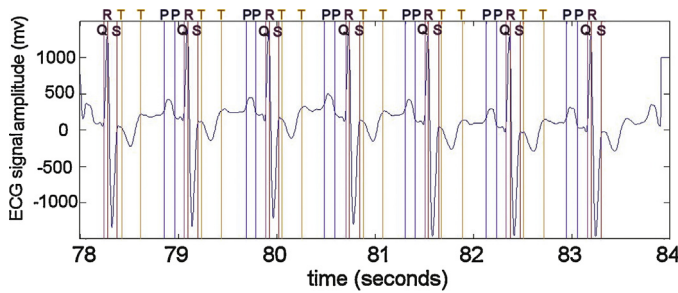
Fig. 9. Typical MATLAB results of the single wave identification process: record 118, data frame: 78–84 s.

the maximum input range of the analogue front-end and transferred to the arbitrary waveform generator which in turn generates the analogue signal to be on-line sampled by the prototype. In on-line data analysis mode, the algorithm is applied continuously over 6-second data sets; the analysis process requires, on average, 2.37E+06 clock cycles per data set. Since the DSP operates on a clock base of 100 MHz, the full analysis process of the 6-second segment is conducted in approximately 2.37 s, while the sampling process continues, thus delivering online, real-time arrhythmia detection results. The LCD display shows on-line analysis results: the heartbeat condition detected, the data segment tested and the classification confidence factor.

4. Results and discussion

Single wave identification is based on detection of maximum and minimum values and zero-crossing detection with respect to the isoelectric line. Fig. 9 shows an example of the graphical summary obtained from the MATLAB single wave identification process.

Table 5 shows a numerical summary of the wave identification results, and the resulting features needed to feed the PNN.

In turn the probabilistic neural network delivers the probability of each arrhythmia considered (Table 6); in this case the highest probability corresponds to RBBB.

Table 6
PNN classification results for record 118, time frame 78–84 s.

Assigned number	Type of arrhytmia	% Probability
1	Auricular fibrillation (AF)	5.0109×10^{-32}
2	Normal sinus rhythm (N)	5.9751×10^{-06}
3	Premature atrial contraction (PVC)	2.0548×10^{-16}
4	Left bundle branch block (LBBB)	1.1939×10^{-04}
5	Right bundle branch block (RBBB)	99.9998
6	Premature ventricular contraction (PVC)	4.0362×10^{-05}
7	Sinoauricular heart block (SHB)	2.8058×10^{-16}
8	Supraventricular tachycardia (SVT)	1.0323×10^{-77}

Fig. 10. Results displayed on LCD in agreement with MATLAB results.

The confidence factor is issued based on the two higher probabilities obtained (23):

$$CF = 1 - e^{-\left(\frac{99.9998 - 1.939E - 04}{1.939E - 04}\right)} \approx 1 \tag{23}$$

which results in a (rounded) 100% confidence factor for RBBB. The results delivered by the prototype are in agreement with those obtained with MATLAB (Fig. 10).

A similar process was applied to 6-s segments of the 17 ECG records to determine the classification accuracy. Upon closer inspection, the data registers in both MATLAB and the prototype are also agreement in all cases, which suggest a similar operation performance (Fig. 11), and thus the results reported here are those delivered by the prototype.

A summary of the results after processing all records is shown in Table 7. Incorrect classification has been identified as misclassified, false positive or false negative. False positive refers to those datasets that were identified as containing an arrhythmic event but correspond to a normal beat; false negatives are those that should have been identified as an arrhythmic event but were catalogued as normal beat. Misclassified data sets are those were an arrhythmic event was identified but corresponds to the wrong type of heartbeat condition.

The accuracy of the QRS detection process has a profound impact on the overall accuracy of the ECG analysis system. The QRS algorithm yielded an overall 99.348% detection success rate. The detection rate difference with respect to other reported methods (Table 8) may be due to the preprocessing operations and the manner in which the programme code is implemented. In addition here the authors used a 6-second data segment that may omit a section of the ECG signal essential for QRS calculation and thus reduce the detection accuracy.

Overall, the classification algorithm appears to yield a considerable high classification performance (i.e. above 97% for records 101 and 119), similar to other reported works.

When a single arrhythmia is present in the test signal, the classification accuracy is high. However, when there is more than one arrhythmia condition present, the classification accuracy degrades.

In order to present the classification results of signals that contain one or more heartbeat conditions, a confusion matrix is used to present correct (and incorrect) classification of a particular class with respect to the rest of the classes, which would further describe the classification performance (Table 9).

The lower scores were obtained for premature atrial contraction and premature ventricular contraction conditions (76.82% and 71.04% respectively). However, the algorithm yielded a 92.69%, 91.94% and 95.45% classification accuracy for auricular fibrillation,
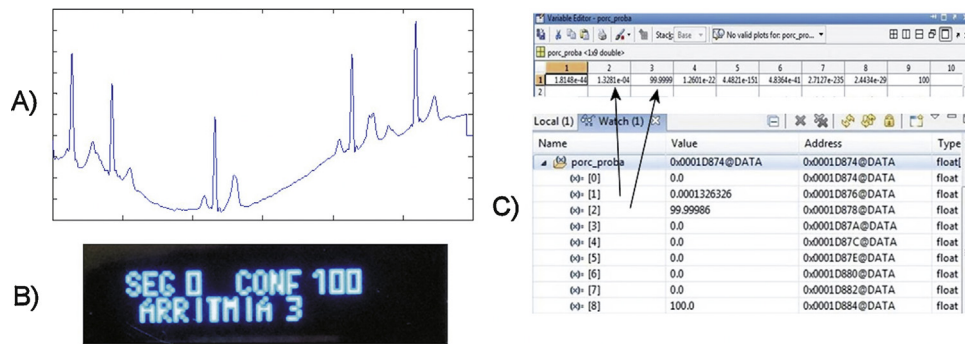
Fig. 11. Numerical result comparison for (A) test signal corresponding to ECG record 201, time frame 18:48–18:54. (B) Prototype results shown on LCD and (C) screen capture of the data registers in MATLAB and C5535-based prototype respectively.

Table 7
Summary of test results, $\sigma^2 = 0.01$.

ECG record	QRS detection	Classification results											
	QRS detection accuracy	Test data set	Correct classification		Failed classification								
					Total number of failed detections		Misclassified		False negative		False positive	
		#	#	%	#	%	#	%	#	%	#	%
100	99.884	287	277	96.516	10	3.484	3	1.045	2	0.697	5	1.742
101	99.778	300	294	98.000	6	2.000	3	1.000	0	0.000	3	1.000
103	99.778	300	288	96.000	12	4.000	2	0.667	0	0.000	10	3.333
105	95.983	278	253	91.007	25	8.993	10	3.597	1	0.360	14	5.036
106	99.808	174	158	90.805	16	9.195	11	6.322	0	0.000	5	2.874
118	99.710	230	203	88.261	27	11.739	25	10.870	0	0.000	2	0.870
119	99.740	192	188	97.917	4	2.083	4	2.083	0	0.000	0	0.000
201	99.012	135	121	89.630	14	10.370	8	5.926	3	2.222	3	2.222
202	99.872	261	239	91.571	22	8.429	9	3.448	4	1.533	9	3.448
203	98.725	170	148	87.059	22	12.941	19	11.176	1	0.588	2	1.176
205	99.882	283	273	96.466	10	3.534	7	2.473	3	1.060	0	0.000
207	99.821	186	171	91.935	15	8.065	14	7.527	0	0.000	1	0.538
209	99.738	254	227	89.370	27	10.630	15	5.906	3	1.181	9	3.543
210	99.753	270	248	91.852	22	8.148	14	5.185	8	2.963	0	0.000
213	98.881	134	120	89.552	14	10.448	5	3.731	7	5.224	2	1.493
215	98.906	198	176	88.889	22	11.111	11	5.556	7	3.535	4	2.020
219	99.579	277	260	93.863	268	96.751	8	2.888	8	2.888	1	0.361
Total	99.344	3929	3644	92.746	285	7.254	168	4.276	47	1.196	70	1.782

#: number of 6-second data segments.
%: percentage referenced to the total number of segments per data set.
Misclassified: heartbeat condition different than normal sinus rhythm detected but classified incorrectly.
False negative: heartbeat considered normal when it should have been classified as arrhythmic beat.
False positive: Normal sinus rhythm wrongly classified as arrhythmic beat.

Table 8
Comparison of QRS detection rate results with results found in the literature.

Author	Processing method	Detection rate
Alexakis et al. [38]	Artificial neural network	87.50%
Alexakis et al. [38]	Linear discriminant analysis	89.96%
Jaswal et al. [27]	Wavelet transform	95.74%
Zeng et al. [24]	Wavelet transform (Mexican hat)	98.21%
Gutierrez et al. [17]	Wavelet transform	98.81%
Ieong et al. [23]	Wavelet transform	99.00%
Zeng et al. [24]	Wavelet transform (Morlet wavelet)	99.20%
Dinh et al. [29]	Wavelet transform	99.25%
Pan et al. [39]	Collection of signal processing techniques	99.33%
This work	Wavelet transform	99.34%
Hamilton and Tompkins [25]	Collection of signal processing techniques	99.46%
Chen et al. [15]	Moving average	99.50%
Alvarado et al. [30]	Wavelet transform	99.53%
Martínez et al. [31]	Wavelet transform	99.66%
Li et al. [44]	Wavelet transform	99.83%

Table 9
Classification results (confusion matrix): percentage.

	AF	N	PAC	LBBB	RBBB	PVC	SHB	SVT
AF	92.69%	1.53%	2.24%	1.18%	0.00%	1.42%	0.00%	0.94%
N	0.64%	97.15%	1.33%	0.23%	0.05%	0.18%	0.37%	0.05%
PAC	9.27%	4.64%	76.82%	0.00%	0.66%	3.97%	4.64%	0.00%
LBBB	0.00%	0.00%	0.00%	91.06%	7.82%	0.56%	0.56%	0.00%
RBBB	1.72%	0.00%	0.86%	6.47%	87.50%	3.45%	0.00%	0.00%
PVC	3.86%	9.27%	12.74%	0.00%	1.16%	71.04%	1.93%	0.00%
SHB	0.00%	8.06%	0.00%	0.00%	0.00%	0.00%	91.94%	0.00%
SVT	0.00%	0.00%	4.55%	0.00%	0.00%	0.00%	0.00%	95.45%

Table 10
ECG arrhythmia classification accuracy comparison.

Author	Processing method	Feature classification	Classification accuracy
This work	Wavelet Transform and Probabilistic Neural Network.	8 heartbeat conditions	92.75%
Ebrahimnezhad et al. [46]	Linear predictive coefficients and Probabilistic Neural Network.	4 heartbeat conditions	92.90%
Tsipouras et al. [34]	Collection of Digital Signal Processing methods.	4 heartbeat conditions	94% (arrhythmic episode) and 98% (arrhythmic beat classification)
Homaeinezhad et al. [37]	Wavelet transform and Fuzzy inference classification (FCM clustering).	QRS geometrical complex	94.58%
de Chazal et al. [35]	Collection of Digital Signal Processing methods.	5 heartbeat conditions	Multiple reports, overall 96.4%
Lin et al. [45]	Wavelet Transform and Probabilistic Neural Network.	7 heartbeat conditions	97% (High) classification rate for a single arrhythmia, decreases when signals contain multiple arrhythmias
Homaeinezhad et al. [37]	Wavelet transform and Fuzzy inference classification (Subtractive clustering).	QRS geometrical complex	97.41%
Yu et al. [47]	Wavelet Transform and Probabilistic Neural Network.	6 heartbeat conditions	99.65%

sinoauricular heart block and atrial fibrillation conditions respectively, when there is more than just a single heart condition present. The performance comparison with other reported works (Table 10) shows a reduced classification accuracy.

However, the data used for testing the ECG classification programme and dedicated hardware, corresponded to a set of analogue signals proceeding from a signal generator, corresponding to the reference ECG database. The classification accuracy obtained and the compact hardware solution used for the experiments, suggest that the method and apparatus described in this work is suitable for implementing on-line real-time arrhythmia classification in wearable sensing applications.

5. Conclusions

Throughout this work it was shown that the inherent nature of the proposed DSP algorithm for arrhythmia classification based on a combination of Wavelet Transform and Probabilistic Neural Network, is suitable for real-time operation on a DSP platform, which in turn is suitable for being implemented on wearable sensing applications. The 6-s data length was selected bearing in mind on-line DSP implementation for delivering real-time information; a complete classification operation is conducted, on average, in approximately 2.4 s, while data is acquired continuously. The classification accuracy of the proposed procedure was initially coded in MATLAB, and tested using data obtained directly from the MIT/BIH records; the classification results where compared to those obtained using the equivalent, digitized, data fed to the DSP-based ECG data acquisition system through the arbitrary waveform generator. The strategy was implemented in order to allow comparison of the classification accuracy, segment by segment, on both MATLAB and DSP-based platforms. The classification results between the DSP prototype and the MATLAB-based programme were 100% in agreement, which contributes to validate the DSP C++ coding procedure. When there is a single arrhythmia present on the test signal, the

overall classification accuracy is high in agreement with reported works. However the results indicate that there is a decreased accuracy when there is more than one arrhythmia condition present; in comparison with previously reported works, the confusion matrix tests classification accuracy, and suggests the decreased detection rate, in particular for PAC and PVC. In contrast, the results may also reflect a more realistic classification performance when compared to the rest of the classes selected. Amongst the factors that may have influenced decreased classification rates are the number of data sets used for training and the presence of other arrhythmia conditions not considered for classification. Another important factor is the accuracy of the QRS algorithm; although the overall classification accuracy is better that 92.74%, there is room for improvement by optimizing the QRS algorithm. On the other hand, the reduced number of electronic components and the overall detection rate of operating on the equivalent, digitized, signals suggest that the method and prototype presented may be suitable for integration into wearable sensing technology, in agreement with current ambulatory sensing trends of technological development which would contribute to early diagnosis.

References

[1] A.S. Adabag, G. Peterson, F.S. Apple, J. Titus, R. King, R.V. Luepker, Etiology of sudden death in the community: results of anatomic, metabolic, and genetic evaluation, Am. Heart. J. 159 (January (1)) (2010) 33–39.
[2] J.J. Goldberger, A.E. Buxton, M. Cain, O. Costantini, D.V. Exner, B.P. Knight, D. Lloyd-Jones, A.H. Kadish, B. Lee, A. Moss, R. Myerburg, J. Olgin, R. Passman, D. Rosenbaum, W. Stevenson, W. Zareba, D.P. Zipes, Risk stratification for arrhythmic sudden cardiac death: identifying the roadblocks, Circulation 123 (2011) 2423–2430.

[3] E. Asensio, R. Narváez, J. Dorantes, J. Oseguera, T.A. Orea, R.P. Hernández, G.V. Rebollar, L. Mont, J. Brugada, Conceptos actuales sobre la muerte súbita, Gac. Med. Mex. 141 (March–April (2)) (2005) 89–98.

[4] M. Velic, I. Padavic, S. Car, Computer aided ECG Analysis – State of the Art and Upcoming Challenges, 2013, arXiv:1306.5096v1 [cs.CV] 21 June.

[5] M.E. Guevara-Valdivia, Monitoreo a distancia de los dispositivos automáticos implantables cardiovasculares (marcapasos, desfibriladores automáticos implantables y resincronizadores cardiacos), Arch. Cardiol. Mex. 79 (July–September (3)) (2009) 221–225.

[6] L. Gatzoulis, I. Iakovidis, Wearable and Portable eHealth Systems: Technological Issues and Opportunities for personalized care, IEEE Eng. Med. Biol. Mag. 26 (September-October (5)) (2007) 51–56.

[7] M. Shapiro, J. Martínez-Sánchez, in: F. Méndez Oteo (Ed.), Arritmias Cardiacas: Introducción a su diagnóstico y tratamiento, 2a ed, 2002, México D.F.

[8] A. Gacek, W. Pedrycz, ECG signal analysis, classification, and interpretation: a framework of computational intelligence, in: A. Gacek, W. Pedrycz (Eds.), ECG Signal Processing, Classification and Interpretation, Springer-Verlag, London, 2012, pp. 47–77.

[9] A. Bayes de Luna, Basic Electrocardiography: Normal and Abnormal ECG Patterns, John Wiley & Sons, New York, 2008.

[10] J. Slocum. A. Sahakian, S.S. Swiiryn, Diagnosis of atrial fibrillation from surface electrocardiograms based on computer-detected atrial activity, J. Electrocardiol. 25 (January (1)) (1991) 1–8, 1992.

[11] F. Bogun, D. Anh, G. Kalahasty, E. Wissner, C.B. Serhal, R. Bazzi, D. Weaver, C. Schuger, Misdiagnosis of atrial fibrillation and its clinical consequences, Am. J. Med. 117 (November (9)) (2004) 636–642.

[12] R.A. Colucci, M.J. Silver, J. Shubrook, Common types of supraventricular tachycardia: diagnosis and management, Am. Fam. Physician 15 (October (8)) (2010) 942–952.

[13] S. Kadambe, R. Murray, G.F. Boudreaux-Bartels, Wavelet transform-based QRS complex detector, IEEE Trans. Biomed. Eng. 46 (July (7)) (1999) 838–848.

[14] D.I. Donoho, J.M. Johnstone, Ideal spatial adaptation via wavelet shrinkage, Biometrika (1994) 425–455.

[15] S.W. Chen, H.C. Chen, H.L. Chan, A real-time QRS detection method based on moving-averaging incorporating with wavelet denoising, Comput. Meth. Prog. Bio. 82 (2006) 187–195.

[16] B.–U. Köhler, C. Hennig, R. Orglmeister, The principles of software QRS detection, IEEE Eng. Med. Biol. Mag. 21 (January–February (1)) (2002) 42–57.

[17] A. Gutiérrez, M. Lara, P.R. Hernandez, A QRS detector based on Haar wavelet, evaluation with MIT-BIH arrhythmia and European ST-T Databases, Comp. Syst. 8 (April–June (4)) (2005) 293–302.

[18] M. Kaneko, T. Gotho, F. Iseri, K. Takeshida, N. Ohki, N. Sueda, QRS complex analysis using wavelet transform and two layered self-organizing map, Comput. Cardiol. 38 (2011) 813–816.

[19] P.S. Addison, Wavelet transforms and the ECG: a review, Physiol. Meas. 26 (2005) R155–R199.

[20] M.J. Burke, M. Nasor, The time relationships of the constituent components of the human electrocardiogram, J. Med. Eng. Technol. 26 (January–February (1)) (2002) 1–6.

[21] A. Schuck, J.O. Wisbeck, QRS detector pre-processing using the complex wavelet transform, in: Proceedings of the 25th Annual International Conference of the IEEE Engineering in Medicine and Biology Society, 17–21 September, (3), 2003, pp. 2590–2593.

[22] V.P. Vassilikos, L. Mantziari, G. Dakos, V. Kamperidis, I. Chouvarda, Y.S. Chatzizisis, P. Kalpidis, E. Theofilogiannakos, S. Paraskevaidis, H. Karvounis, S. Mochlas, N. Maglaveras, I.H. Styliadis, QRS analysis using wavelet transformation for the prediction of response to cardiac resynchronization therapy: a prospective pilot study, J. Electrocardiol. 47 (January–February 1) (2014) 59–65.

[23] C.–I. Ieong, P.–I. Mak, C.–P. Lam, C. Dong, A 0.83-μW QRS detection processor using quadratic spline wavelet transform for wireless ECG Acquisition in 0.35-μm CMOS, IEEE Trans. Biomed. Circuits Syst. 6 (December 6) (2012) 586–595.

[24] C. Zeng, H. Lin, Q. Jiang, M. Xu, QRS complex detection using combination of Mexican-hat wavelet and complex Morlet wavelet, J. Comput. 8 (November 11) (2013) 2951–2958.

[25] P.S. Hamilton, W.J. Tompkins, Quantitative investigation of QRS detection rules using the MIT/BIH arrhythmia database, IEEE Trans. Bio-Med. Eng. BME 33 (December (12)) (1986) 1157–1165.

[26] M. Okada, A digital filter for the QRS complex detection, IEEE Trans. Bio-Med. Eng. BME 26 (December (12)) (1979) 700–703.

[27] G. Jaswal, R. Parmar, A. Kaul, QRS detection using wavelet transform, Int. J. Eng. Adv. Tech. 1 (August 6) (2012) 1–5.

[28] H.H. So, K.L. Chan, Development of QRS detection method for real-time ambulatory cardiac monitor, in: Proceedings of the 19th Annual International Conference of the IEEE Engineering in Medicine and Biology Society, Oct. 30 1997–Nov. 2 1997, 1, 1997, pp. 289–292.

[29] H.A.N. Dinh, D.K. Kumar, N.D. Pah, P. Burton, Wavelets for QRS detection, in: Proceedings of the 23rd IEEE Annual International Conference of the IEEE Engineering in Medicine and Biology Society, Oct. 25–28, Istanbul, Turkey, Vol. 2, 2001, pp. 1883–1887.

[30] C. Alvarado, J. Arregui, J. Ramos, R. Pallás-Areny, Automatic detection of ECG ventricular activity waves using continuous spline wavelet transform, in: Proceedings of the 2nd International Conference on Electrical and Electronics Engineering (ICEEE) and XI Conference on Electrical Engineering (CIE 2005), Mexico City, Mexico, September 7–9, 2005, pp. 189–192.

[31] J.P. Martínez, R. Almeida, S. Olmos, A.P. Rocha, P. Laguna, A wavelet-based ECG delineator: evaluation on standard databases, IEEE Trans. Bio-Med. Eng. 51 (April (4)) (2004) 570–581.

[32] M.S. Manikandan, K.P. Soman, A novel method for detecting R-peaks in electrocardiogram (ECG) signal, Biomed. Signal Process. 7 (March (2)) (2012) 118–128.

[33] H. Atoui, J. Fayin, P. Rubel, A neural network approach for patient-specific 12-lead ECG synthesis in patient monitoring environments, in: Proceedings IEEE Computers in Cardiology, 2004, pp. 161–164.

[34] M.G. Tsipouras, D.I. Fotiadis, D. Sideris, An arrhythmia classification system based on the RR-interval signal, Artif. Intell. Med. 33 (March (3)) (2005) 237–250.

[35] P. de Chazal, M. O'Dwyer, R.B. Reilly, Automatic classification of heartbeats using ECG morphology and heartbeat interval features, IEEE Trans. Bio-Med. Eng. 51 (July (7)) (2004) 1196–1206.

[36] P. Laguna, R. Jané, P. Caminal, Automatic detection of wave boundaries in multilead ECG signals: validation with the CSE database, Comput. Biomed. Res. 27 (February (1)) (1994) 45–60.

[37] M.R. Homaeinezhad, E. Tavakkoli, A. Ghaffari, Discrete wavelet-based fuzzy network architecture for ECG rhythm-type recognition: feature extraction and clustering-oriented tuning of fuzzy inference system, Int. J. Signal Process. Image Process. Pattern Recogn. 4 (September (3)) (2011) 107–129.

[38] C. Alexakis, H.O. Nyongesa, R. Saatchi, N.D. Harris, C. Davies, C. Emery, R.H. Ireland, S.R. Heller, Feature extraction and classification of electrocardiogram (ECG) signals related to hypoglycaemia, Proc. Comput. Cardiol. 30 (2003) 537–540.

[39] J.J. Pan, W.J. Tompkins, A real-time QRS detection algorithm, IEEE Trans. Bio-Med. Eng. BME 32 (March (3)) (1985) 230–236.

[40] Y. Sun, S. Suppappola, T.A. Wrublewski, Microcontroller-based real-time QRS detection, Biomed. Inst. Technol. 26 (December (6)) (1992) 477–484.

[41] S. Karpagachelvi, M. Arthanari, M. Sivakumar, ECG feature extraction techniques – a survey approach, Int. J. Comput. Sci. Inf. Security 8 (April 1) (2010) 76–80, aRxiv:1005.0957 [cs.NE].

[42] J.A. Gutierrez-Gnecchi, R. Morfin-Magaña, A. del, C. Tellez-Anguiano, D. Lorias-Espinoza, E. Reyes-Archundia, O. Hernandez-Diaz, Cardiac arrhythmia classification using a combination of quadratic spline wavelet transform and artificial neural classification network, in: Proceedings of the 2nd International Work-Conference on Bioinformatics and Biomedical Engineering, Granada, Spain, April 7th–9th, 2014, pp. 1743–1754.

[43] S. Mallat, W.L. Hwang, Singularity detection and processing with wavelets, IEEE Trans. Inform. Theory 38 (March (2)) (1993) 617–643.

[44] C. Li, C. Zheng, C. Tai, Detection of ECG characteristic points using wavelet transforms, IEEE Trans. Bio-Med. Eng. 42 (January (1)) (1995) 21–28.

[45] C.H. Lin, Y.C. Du, T. Chen, Adaptive wavelet network for multiple cardiac arrhythmias recognition, Expert Syst. Appl. 34 (May 4) (2008) 2601–2611.

[46] H. Ebrahimnezhad, S. Khoshnoud, Classification of arrhythmias using linear predictive coefficients and probabilistic neural network, Appl. Med. Inf. 33 (September (3)) (2013) 55–62.

[47] S.N. Yu, Y.H. Chen, Electrocardiogram beat classification based on wavelet transformation and probabilistic neural network, Pattern Recogn. Lett. 28 (2007) 1142–1150.

[48] A.L. Goldberger, L.A.N. Amaral, L. Glass, J.M. Hausdorff, P.Ch. Ivanov, R.G. Mark, J.E. Mietus, G.B. Moody, C.K. Peng, H.E. Stanley, PhysioBank, PhysioToolkit, and PhysioNet: components of a new research resource for complex physiologic signals, Circulation 101 (June (23)) (2000) e215–e220.

[49] G.B. Moody, R.G. Mark, The impact of the MIT BIH arrhythmia database, IEEE Eng. Med. Biol 20 (May–June (3)) (2001) 45–50.

[50] S.G. Mallat, A theory for multiresolution signal decomposition: the wavelet representation, IEEE Trans. Pattern Anal. 11 (July (7)) (1989) 674–693.

[51] S. Mallat, Multifrequency channel decompositions of images and wavelet models, IEEE Trans. Acoust. Signal Process. 37 (December (12)) (1989) 2091–2110.

[52] N.V. Thakor, J.G. Webster, W.J. Tompkins, Estimation of QRS complex power spectra for design of a QRS filter, IEEE Trans. Bio-Med. Eng. BME-31 (November (11)) (1984) 702–706.